



Spray evaporative cooling to achieve ultra fast cooling in runout table

P. Bhattacharya*, A.N. Samanta, S. Chakraborty

Department of Chemical Engineering, Indian Institute of Technology Kharagpur, Kharagpur – 721302 West Bengal, India

ARTICLE INFO

Article history:

Received 25 March 2008
 Received in revised form
 1 September 2008
 Accepted 23 January 2009
 Available online 21 March 2009

Keywords:

Spray evaporative cooling (SEC)
 Droplet evaporation time
 Critical droplet size
 Ultra Fast Cooling (UFC)
 Runout Table (ROT)
 Discrete Phase Model (DPM)

ABSTRACT

Spray evaporative cooling, in lieu of conventional laminar jet impingement cooling, has potential to achieve the anomalously high strip cooling rate of Ultra Fast Cooling – 300 °C/s for a 4 mm thick carbon steel strip – in Runout Table of Hot Strip Mill. In the present study, evaporation time of a single droplet impinging on a hot carbon steel strip surface has been analytically evaluated as a function of droplet diameter from fundamental heat transfer perspective based on the premise that a spray can be considered as a multi-droplet array of liquid at low spray flux density. Droplet evaporation time thus evaluated has been used to estimate strip cooling rate achievable in Runout Table of Hot Strip Mill by spray evaporative cooling. The proposed analytical model predicts that it is indeed possible to achieve the ultra-high cooling rate of Ultra Fast Cooling by spray evaporative cooling by suitable reduction of droplet size. A general analytical expression has also been developed to estimate critical droplet size to achieve Ultra Fast Cooling as a function of steel strip thickness. Predictions of the analytical model have been validated using CFD simulation with a modified Discrete Phase Model.

© 2009 Elsevier Masson SAS. All rights reserved.

1. Introduction

Spray evaporative cooling (SEC) is a very promising thermal management technique for high heat flux applications like Runout Table cooling in Hot Strip Mill. SEC has capability to achieve significantly higher heat flux compared to pool boiling due to reduction in resistance to vapor removal from heated surface. Heat fluxes as high as 10 MW/m² with SEC has been reported in [1]. SEC is characterized by uniformity of heat removal and small fluid inventory which makes it an appealing choice for many cooling systems. Overall theoretical understanding of SEC is still in its infancy due to complex interaction of liquid and vapor phases, liquid droplet impact and phase change.

Spray evaporative cooling can be used as an alternative to conventional laminar jet impingement cooling for Runout Table (ROT) cooling in Hot Strip Mill (HSM). Within HSM, steel slabs from continuous slab casting process are hot-rolled into thinner and longer strips by rolls that is ultimately led to ROT. ROT acts as a metallurgical tool to provide desired cooling rate to obtain appropriate product. It is to be noted that high strength steel necessitates development of multiphase microstructures (like ferrite–bainite, ferrite–martensite etc.) which is difficult on a conventional ROT equipped with laminar cooling technology.

Alloying with elements like manganese, chromium and molybdenum becomes necessary to generate the complex microstructures. CRM's Ultra Fast Cooling (UFC) technology has capability to produce fine grain high strength steel at low cost by reducing the consumption of alloying elements. Development and implementation of UFC has been reported by Lucas et al. [2] and Herman [3].

Ultra Fast Cooling (UFC) in Hot Strip Mill entails cooling rate of about 300 °C/s which corresponds to heat transfer rate of 4.37 MW for a 4 mm thick carbon steel strip. The cooling rate obtained is an order of magnitude higher than conventional laminar jet cooling. We have not come across the method to achieve the anomalously high strip cooling rate with UFC in open literature. Using spray evaporative cooling instead of conventional laminar jet impingement cooling might help to achieve the ultra-high strip cooling rate of UFC.

Due to the high strip temperature in Runout Table – ranging between 700 and 1100 °C at entry point – droplet evaporation corresponds to film evaporation regime whereby the droplet loses contact with the hot strip surface and levitates above its own vapor. Droplet evaporation rate is affected by many interdependent parameters. However for simplicity and ease of mathematical treatment, we have only considered the effect of droplet diameter and impinging surface temperature in the analytical model.

Literature review reveals several studies related to conventional laminar jet impingement cooling in Runout Table. Hatta and Osakabe [4] numerically modeled cooling process of a horizontally

* Corresponding author. Tel.: +91 3222 283948.

E-mail address: prasenjit@che.iitkgp.ernet.in (P. Bhattacharya).

Nomenclature		ΔT	strip surface superheat ($=T_{\text{strip}} - T_{\text{sat}}$) ($^{\circ}\text{C}$)
a	capillary length (m)	$(-dT/dt)_{\text{strip}}$	strip cooling rate ($^{\circ}\text{C/s}$)
A_d	contact area of droplet (m^2)	$(-dT/dt)_{\text{UFC}}$	strip cooling rate for UFC ($^{\circ}\text{C/s}$)
A_{strip}	surface area of steel strip (m^2)	w	spray flowrate [lpm (liters per minute)]
B	constant, in Eq. (3)	Greek symbols	
C_0	coefficient, in Eq. (9)	δ_{strip}	thickness of steel strip (mm)
C_p	specific heat (J/kg K)	μ	viscosity (kg/ms)
D	instantaneous diameter of droplet (μm (micrometer))	ν	surface tension (N/m)
D_0	initial diameter of droplet (μm)	ρ	density (kg/m^3)
$D_{0,\text{cr}}$	critical droplet size (μm)	σ	Stefan-Boltzmann constant ($\text{W/m}^2 \text{K}^4$)
e	vapor film thickness (μm)	Subscripts	
g	acceleration due to gravity (m/s^2)	cond	conductive
h	heat transfer coefficient (HTC) ($\text{W/m}^2 \text{K}$)	sat	saturation
h_{fg}	latent heat of evaporation (J/kg)	strip	steel strip
k	thermal conductivity (W/mK)	v	vapor
m_d	mass of droplet (kg)	p	discrete droplet phase
$-dm_d/dt$	droplet evaporation rate (kg/s)	∞	continuous gas phase
n	surface renewal rate (frequency) ($=1/t_{\text{evap}}$) (s^{-1})	cr	critical
N	site density (no of droplets per unit area of strip) (m^{-2})	d	droplet
q''	heat flux (W/m^2)	hemi	hemispherical
r	instantaneous radius of droplet (μm)	l	liquid
r_0	initial radius of droplet (μm)	net	net (total)
Re	Reynolds number	o	initial
t	instantaneous time (s)	rad	radiative
t_{evap}	droplet evaporation time (s)		
T	temperature ($^{\circ}\text{C}$)		

moving hot steel plate by a laminar water curtain. Fujimoto et al. [5] numerically simulated transient cooling of a hot solid by an impinging circular free surface liquid jet. Timm et al. [6] presented an analytical approach for heat transfer in subcooled jet impingement boiling at high wall temperature. Hauksson et al. [7] experimentally studied boiling heat transfer during subcooled water jet impingement on flat steel surface. However studies related to spray evaporative cooling in the context of Runout Table cooling are lacking in the literature.

In the present paper, an analytical expression of evaporation time for a single droplet undergoing film evaporation on a heated surface has been developed as a function of droplet diameter and impinging surface temperature from fundamental heat transfer perspective based on the premise that a spray is equivalent to a multi-droplet array of liquid at sufficiently low spray flux density where droplet-to-droplet interaction can be neglected. The ultimate objective is to verify whether it is at all possible to achieve the anomalously high strip cooling rate of Ultra Fast Cooling in Runout Table of Hot Strip Mill by spray evaporative cooling. We have not come across similar analytical approach to estimate strip cooling rate in Runout Table. A general analytical expression has also been developed to estimate critical droplet size to achieve Ultra Fast Cooling as a function of steel strip thickness. Predictions of the analytical model have been validated using CFD simulation with a modified Discrete Phase Model.

2. Model formulation

2.1. Analytical model

Fig. 1 depicts a schematic of the analytical model developed to estimate droplet evaporation time. Spherical water droplet spreads and forms a hemispherical droplet of same volume upon impingement on the hot carbon steel strip surface.

2.1.1. Assumptions

- 1 Spherical droplet has reached the saturation temperature of water by the time it impinges on the hot strip surface.
- 2 Superheating of generated vapor is ignored. Thus phase change of water alone accounts for the cooling of steel strip.
- 3 Spray flux density is controlled such that complete evaporation of water droplet occurs.
- 4 Recoil, splashing and disintegration of droplet upon impingement on the hot steel strip surface are neglected.
- 5 Vapor film is assumed to be at a temperature midway between strip temperature and saturation temperature of water.
- 6 Curved surface of hemispherical droplet is thermally insulated.

2.1.2. Derivation of analytical expression for droplet evaporation time

An analytical expression for droplet evaporation time has been derived from overall energy balance. Evaporation rate can be expressed as in Eq. (1):

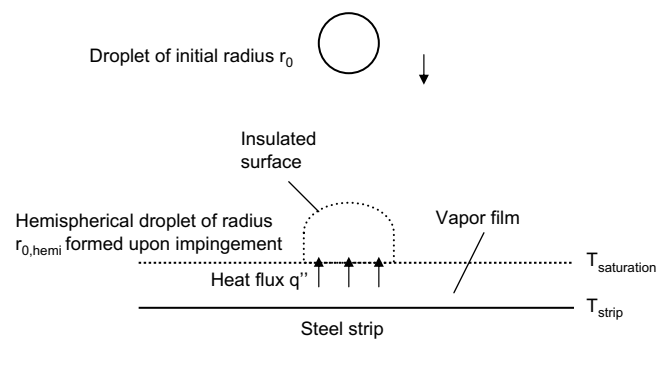


Fig. 1. Schematic of analytical model.

$$q''_{\text{net}} A_d = (-dm_d/dt) h_{fg} \quad (1)$$

Heat transfer from steel strip surface to water droplet takes place through the flat surface of the hemispherical droplet which is in contact with the vapor film. This heat provides the latent heat of vaporization for the entire droplet so that the entire droplet shrinks in size with time. Thus Eq. (1) simplifies to Eq. (2):

$$q''_{\text{net}} (\pi r_{\text{hemi}}^2) = - \left[\frac{d}{dt} \left(\frac{2}{3} \pi r_{\text{hemi}}^3 \rho_l \right) \right] h_{fg} \quad (2)$$

Evaluation of the derivative and simplification of Eq. (2) yields droplet shrinkage rate as in Eq. (3):

$$-\frac{dr_{\text{hemi}}}{dt} = \frac{q''_{\text{net}}}{2\rho_l h_{fg}} = B \quad (3)$$

Right hand side of Eq. (3) is a constant (denoted as B). Thus the following integration can be carried out to yield an expression for droplet evaporation time as in Eq. (4):

$$\begin{aligned} - \int_{r_{0,\text{hemi}}}^0 dr_{\text{hemi}} &= B \int_0^{t_{\text{evap}}} dt \Rightarrow r_{0,\text{hemi}} = B t_{\text{evap}} \Rightarrow t_{\text{evap}} = \frac{r_{0,\text{hemi}}}{B} \\ &= \frac{D_{0,\text{hemi}}}{2B} \end{aligned} \quad (4)$$

Initial diameter of the flattened hemispherical droplet in Eq. (4) can be estimated using equality of volume as in Eq. (5):

$$\frac{\pi}{12} D_{0,\text{hemi}}^3 = \frac{\pi}{6} D_0^3 \Rightarrow D_{0,\text{hemi}} = \sqrt[3]{2} D_0 \quad (5)$$

Water droplet levitates on the vapor film that separates the steel strip from the droplet. Heat transfer from steel strip to water droplet takes place by conduction through the vapor film as well as radiation. Thus net heat flux in Eqs. (1)–(4) can be expressed as in Eq. (6):

$$q''_{\text{net}} = q''_{\text{cond}} + q''_{\text{rad}} \quad (6)$$

Conductive heat flux in Eq. (6) can be expressed as in Eq. (7):

$$q''_{\text{cond}} = \frac{k_v (T_{\text{strip}} - T_{\text{sat}})}{e} \quad (7)$$

Radiative heat flux in Eq. (6) can be expressed using Stefan-Boltzmann law as in Eq. (8):

$$q''_{\text{rad}} = \sigma (T_{\text{strip}}^4 - T_{\text{sat}}^4) \quad (8)$$

Vapor film thickness (e) is required to evaluate conductive heat flux in Eq. (7). This has been estimated using Eq. (9) as in Bianci et al. [8]. It has been assumed that vapor film thickness depends only upon initial droplet diameter and strip surface superheat and remains constant during the course of droplet evaporation.

$$e \sim \left(\frac{k_v \Delta T \mu_v \rho_l g}{h_{fg} \rho_v \gamma^2} \right)^{1/3} D_0^{4/3} \Rightarrow e = C_0 \times (T_{\text{strip}} - T_{\text{sat}})^{1/3} (D_0)^{4/3} \quad (9)$$

All variables in Eq. (9) are in SI units. It is to be noted that vapor film thickness changes with droplet diameter as (diameter)^{1/2} for puddles and (diameter)^{4/3} for droplets smaller than capillary length [8]. Thus Eq. (9) holds provided the inequality in Eq. (10) is satisfied:

$$D_0 < 2a \quad (10)$$

where the capillary length (a) is given by Eq. (11):

$$a = \left(\frac{\gamma}{\rho_l g} \right)^{1/2} \quad (11)$$

The coefficient term C_0 in Eq. (9) has been estimated from the experimental data of Xiong and Yuen [9]. The data point for evaporation lifetime of water droplet of diameter 500 μm impinging on a stainless steel surface at 520 °C has been used since this is above the Leidenfrost temperature of water (around 280 °C) and the present study also pertains to film evaporation regime. This yields a value of 0.212 for C_0 in Eq. (9) if all variables are expressed in SI units. It is to be noted that the experimental data in [9] pertains to droplet evaporation on a stainless steel surface whereas the present study involves droplet evaporation on a carbon steel surface. However surface material does not affect droplet evaporation time in film evaporation regime as noted by Michiyoshi and Makino [10].

2.1.3. Derivation of analytical expression for critical droplet size

After estimation of droplet evaporation time (t_{evap}) using Eq. (4) in conjunction with Eq. (3) and Eqs. (5)–(9), cooling load for Ultra Fast Cooling (UFC) can be estimated using Eq. (12). This equation will be the starting point to analytically evaluate critical droplet size ($D_{0,\text{cr}}$) to achieve Ultra Fast Cooling as a function of steel strip thickness. It is to be noted that the carbon steel strip is spray cooled from both sides.

Cooling load for UFC

= Heat removed per droplet

× Surface renewal rate

× Site density $\Rightarrow (A \delta \rho C_p)_{\text{strip}} \left(-\frac{dT}{dt} \right)_{\text{UFC}} = (m_d \times h_{fg})$

× $\frac{1}{t_{\text{evap}}} \times (2 \times N)$ (12)

Substituting for t_{evap} from Eq. (4) and simplification of Eq. (12) for a 1 m² steel strip surface yields Eq. (13):

$$\begin{aligned} [(\rho C_p)_{\text{strip}} \left(-\frac{dT}{dt} \right)_{\text{UFC}}] \delta_{\text{strip}} &= \left[\left(\frac{\pi}{6} D_0^3 \rho_l \right) \times h_{fg} \right] \\ &\times \frac{2B}{D_{0,\text{hemi}}} \times \left(2 \times \frac{1}{D_{0,\text{hemi}}^2} \right) \end{aligned} \quad (13)$$

Substituting for B from Eq. (3) and $D_{0,\text{hemi}}$ from Eq. (5), Eq. (13) simplifies to Eq. (14):

$$\left[(\rho C_p)_{\text{strip}} \left(-\frac{dT}{dt} \right)_{\text{UFC}} \right] \delta_{\text{strip}} = \frac{\pi}{6} q''_{\text{net}} \quad (14)$$

Substituting for q''_{net} using Eqs. (6)–(9), Eq. (14) simplifies to Eq. (15):

$$\begin{aligned} \left[(\rho C_p)_{\text{strip}} \left(-\frac{dT}{dt} \right)_{\text{UFC}} \right] \delta_{\text{strip}} &= \frac{\pi}{6} \left[\frac{k_v (T_{\text{strip}} - T_{\text{sat}})^{2/3}}{C_0 D_{0,\text{cr}}^{4/3}} \right. \\ &\left. + \sigma (T_{\text{strip}}^4 - T_{\text{sat}}^4) \right] \end{aligned} \quad (15)$$

Eq. (15) is the general equation relating critical droplet size ($D_{0,\text{cr}}$) with steel strip thickness (δ_{strip}). Critical droplet size indicates the droplet diameter needed to provide desired cooling rate of Ultra Fast Cooling (300 °C/s) for a particular thickness of steel strip. Ignoring radiative heat flux, Eq. (15) yields Eq. (16) after rearrangement:

$$\delta_{\text{strip}} D_{0,\text{cr}}^{4/3} = \left[\frac{(\pi/6)(k_v/C_0)}{(\rho C_p)_{\text{strip}} (-dT/dt)_{\text{UFC}}} \right] (T_{\text{strip}} - T_{\text{sat}})^{2/3} \quad (16)$$

With the parameters as in Table 1 and for a fixed strip surface superheat of 800 °C, Eq. (16) simplifies to Eq. (17):

$$\delta_{\text{strip}} D_{0,\text{cr}}^{4/3} = 11.534 \times 10^{-9} \quad (17)$$

All variables in Eq. (17) are in SI units. If steel strip thickness is expressed in mm and critical droplet size in μm , Eq. (17) yields Eq. (18):

$$\delta_{\text{strip}}(\text{mm}) [D_{0,\text{cr}}(\mu\text{m})]^{4/3} = 1153.4 \quad (18)$$

Eq. (18) has been used to plot critical droplet size as a function of steel strip thickness in Fig. 4.

2.2. CFD model for validation

Droplet evaporation time estimated by the analytical model has been validated using CFD (Computational Fluid Dynamics) simulation with Discrete Phase Model (DPM). Commercial finite volume software package FLUENT ver 6.2.16 [11] has been used for the simulation. It is to be noted that DPM Model was originally developed for spray drying applications where heat transfer takes place from hot gas phase to liquid droplet phase. As such, this model is not suited for spray evaporative cooling in Hot Strip Mill where heat transfer takes place from heated solid surface to liquid phase. An attempt has been made to simulate heat transfer from hot steel strip surface in Runout Table to water droplet using DPM multiphase model of FLUENT with suitable modifications so as to estimate droplet evaporation time.

2.2.1. Overview of DPM model

In addition to solving transport equations for the continuous gas phase, FLUENT allows simulation of a discrete second phase in a Lagrangian frame of reference. This second phase can consist of spherical droplets dispersed in continuous phase. FLUENT computes heat and mass transfer to/from these discrete phase entities. The coupling between phases and its impact on both discrete phase trajectories and continuous phase flow can be included. Discrete phase formulation assumes that second phase is sufficiently dilute so that particle–particle interaction and effect of particle volume fraction on gas phase are negligible which in turn implies that discrete phase must be present at fairly low volume fraction usually less than 10–12%. Discrete phase can be included in

Table 1
Base input conditions.

<i>For carbon steel strip</i>	
Density (kg/m^3) [13]	7833
Specific heat (J/kg K) [13]	465
Thickness	4 mm
Surface area	1 m \times 1 m
Temperature	900 °C
Desired cooling rate of UFC	300 °C/s
<i>For water at atmospheric pressure</i>	
Saturation temperature (T_{sat})	100 °C
Density at T_{sat} (kg/m^3) [13]	960.6
Thermal conductivity at T_{sat} (W/m K) [13]	0.68
Latent heat of evaporation (J/kg)	2,257,000
Surface tension at T_{sat} (N/m) [13]	0.0588
Thermal conductivity of water vapor at mean temp 500 °C (W/m K) [13]	0.0592
Specific heat of water vapor at mean temp 500 °C (J/kg K) [13]	2152
Viscosity of water vapor at mean temp 500 °C (kg/ms) [13]	27.86×10^{-6}
<i>Constants</i>	
Stefan-Boltzmann constant ($\text{W/m}^2 \text{K}^4$)	5.67×10^{-8}
Acceleration due to gravity (m/s^2)	9.81
Coefficient C_0 in Eq. (9)	0.212

the model by defining initial position, velocity, size and temperature of individual particles. These initial conditions along with inputs defining physical properties of discrete phase are used to initiate heat/mass transfer calculations, which are based on convective heat and mass transfer from the particle using local continuous phase conditions as the particle moves through the flow. The predicted heat and mass transfer can be viewed graphically and/or alphanumerically [11].

2.2.2. Choice of DPM boundary condition at strip surface

Wall-jet DPM boundary condition has been prescribed at the strip surface. Wall-jet signifies that direction and velocity of droplets are given by resulting momentum flux. Wall-jet boundary condition assumes an analogy with an inviscid jet impacting a solid wall. Wall-jet boundary condition is appropriate for high-temperature walls like steel strip surface in Runout Table where no significant liquid film is formed and in high-Weber-number impacts where spray acts as a jet [11].

2.2.3. Heat transfer modeling using DPM model

DPM model in FLUENT has been suitably modified to simulate heat transfer from hot solid steel strip to liquid droplet and to be inline with the assumptions of the analytical model developed in the preceding subsection. Droplet at saturation temperature impinges on the heated strip surface at a velocity of 0.4 m/s to be in sync with the experimental data in Xiong and Yuen [9]. Droplet injection frequency is controlled to prevent droplet–droplet interaction by setting the particle time-step to 5 s which is much higher than the maximum value of droplet evaporation time in the present study. Evaporation is allowed to start only after the droplet strikes the wall. Fluid layer adjacent to wall is maintained at strip temperature throughout the evaporation process. This layer is assumed to be entirely comprised of water vapor. Only boiling law [11] is activated as the discrete phase droplet at saturation temperature is in boiling state. Droplet progressively shrinks in size as it rolls along the surface and completely evaporates before it exits the domain.

Boiling law [11] used by DPM model is given below in Eq. (19). Heat transfer is bi-directional so that latent heat of evaporation of discrete droplet phase appears as an energy sink term in energy equation of continuous gas phase.

$$\begin{aligned} -\frac{dm_d}{dt} h_{\text{fg}} &= hA(T_\infty - T_p) \Rightarrow \frac{dD_p}{dt} \\ &= \frac{4k_\infty}{\rho_p C_{p\infty} D_p} \left(1 + 0.23\sqrt{\text{Re}}\right) \times \ln \left[1 + \frac{C_{p\infty}(T_\infty - T_p)}{h_{\text{fg}}}\right] \end{aligned} \quad (19)$$

2.2.4. Solution methodology

In DPM model, discrete droplet phase is simulated in a Lagrangian frame of reference while transport equations are solved for the continuous gas phase. Solution methodology involves the following three steps [11]:

- 1 Discrete phase injections created. Initial conditions set.
- 2 Flow field initialized.
- 3 Solution advanced in time. Status of droplets updated at the end of each time-step.

Segregated unsteady solver has been used with second order implicit formulation. PISO scheme (Pressure-Implicit with Splitting of Operators) has been used for pressure–velocity coupling. Second order upwind scheme has been used for discretization of momentum, species and energy equations to minimize numerical

Table 2
Predictions of analytical model for base input conditions.

Droplet diameter (μm)	Droplet evaporation time (s)	Surface renewal rate (s ⁻¹)	Spray flowrate (lpm)	Cooling load (MW)	Strip Cooling rate (°C/s)
200	0.252	4	31.7	1.14	79
100	0.051	19	75.2	2.72	187
50	0.0103	97	192	6.94	476
70	0.0227	44	121.9	4.4	302

errors. Under-relaxation factors for the update of computed variables at each iteration are for pressure = 0.2, momentum = 0.5, species H₂O = 0.8, species O₂ = 1, discrete phase sources = 0.5 and energy = 1. Convergence is judged by energy residual falling below 10⁻⁶ and all other residuals (namely continuity, velocity components and species) below 10⁻³. Change of droplet diameter with time has been tracked in FLUENT alphanumerically using: Particle tracks → Color by particle diameter. Fig. 6 depicts this change for a 70 μm water droplet.

3. Results and discussions

3.1. Analytical model

Droplet evaporation time has been estimated for different droplet diameters for a fixed steel strip thickness of 4 mm using Eq. (4) in conjunction with Eq. (3) and Eqs. (5)–(9). Strip thickness of 4 mm corresponds to base input condition to be inline with the plant data for UFC reported by Lucas et al. [2] and Herman [3]. The estimated droplet evaporation time for different droplet sizes using the present model has been used to calculate strip cooling rate achievable by spray evaporative cooling using Eq. (20):

$$\left(\frac{dT}{dt}\right)_{\text{strip}} = \frac{(m_d \times h_{fg}) \times \frac{1}{t_{\text{evap}}} \times (2 \times N)}{(A\delta\rho C_p)_{\text{strip}}} \quad (20)$$

Input data for the calculations is given in Table 1. The results are summarized in Table 2 for base input conditions. It is observed that it is indeed possible to achieve the ultrahigh strip cooling rate of Ultra Fast Cooling – 300 °C/s for a 4 mm thick carbon steel strip as reported in [2] and [3] – by reducing the droplet size to 70 μm although film evaporation takes place due to high strip temperature. It is to be noted that the analytical model assumes that droplet

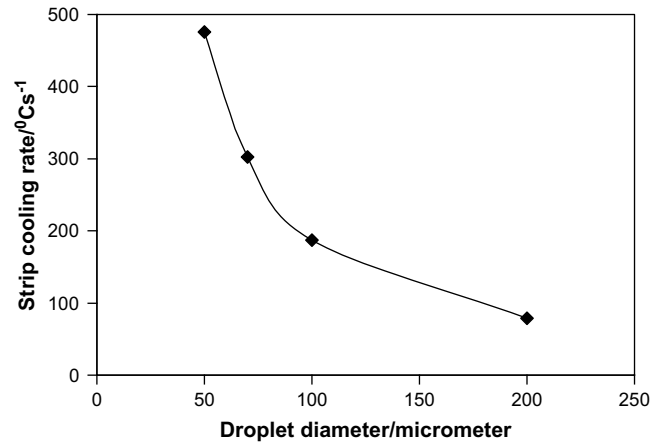


Fig. 3. Variation of strip cooling rate with droplet diameter.

injection frequency is controlled so that next droplet strikes the strip surface only after the first droplet has completely evaporated i.e. droplet injection frequency (surface renewal rate) is equal to inverse of droplet evaporation time. Spray flowrate (droplet density) in Table 2 has been calculated based upon this assumption using Eq. (21):

$$\begin{aligned} \text{Spray flowrate} &= \text{Mass of each droplet} \\ &\times \text{Surface renewal rate} \times \text{Site density} \\ &= m_d \times \frac{1}{t_{\text{evap}}} \times (2 \times N) \end{aligned} \quad (21)$$

After obtaining spray flowrate from Eq. (21), cooling load in Table 2 has been calculated by multiplying spray flowrate with latent heat of vaporization. It is to be noted that the analytical model has ignored the effect of impinging velocity of droplet (or Weber number) since the emphasis of the study is on heat transfer through phase change. Effect of droplet impinging velocity will be important for forced convection cooling.

Fig. 2 depicts the dependence of evaporation time on droplet diameter whereas Fig. 3 depicts the dependence of steel strip cooling rate on droplet diameter for the 4 mm thick steel strip. As expected, droplet evaporation time decreases and consequently strip cooling rate increases in a non-linear fashion with decrease of droplet diameter. This is because smaller droplets have higher specific surface area and produce thinner vapor film on hot strip surface. Even for relatively coarse droplet of diameter 200 μm, the model predicts strip cooling rate as 79 °C/s which is much higher than that achievable in conventional laminar jet cooling – about 15–20 °C/s [3].

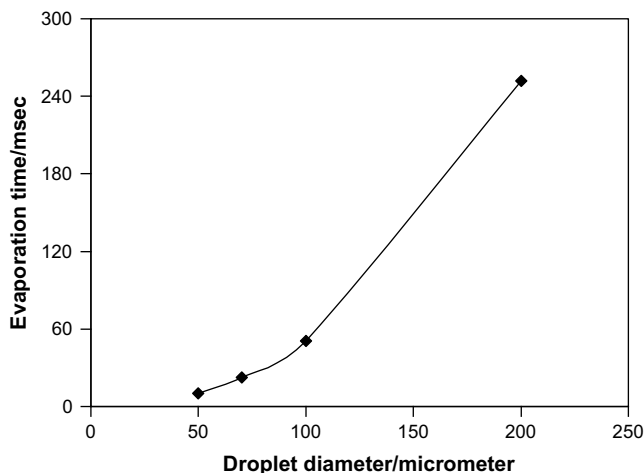


Fig. 2. Variation of evaporation time with droplet diameter.

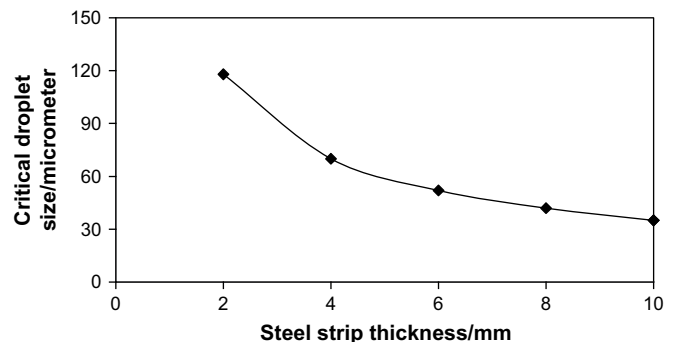


Fig. 4. Effect of steel strip thickness on critical droplet size.

Table 3
Validation of analytical model using CFD simulation for base input conditions.

Droplet diameter (μm)	Droplet evaporation time (s)	
	Analytical model	CFD simulation
200	0.252	0.280
100	0.051	0.075
50	0.0103	0.020
70	0.0227	0.037

The results discussed so far pertains to 4 mm thick carbon steel strip. Fig. 4 depicts the effect of steel strip thickness on critical droplet size to achieve Ultra Fast Cooling (UFC). Critical droplet size has been estimated using Eq. (18). Based upon previous discussion, critical water droplet size for 4 mm thick carbon steel strip is 70 μm . Fig. 4 shows that critical droplet size decreases as steel strip thickness increases. Thus smaller droplets may be capable of providing the increased cooling load to achieve UFC for thicker steel strips. For very thick strips, NanoMist can be an option to provide desired cooling rate of UFC. However it is to be realized that energy cost of atomization also increases as droplet size decreases.

3.2. CFD validation

Droplet evaporation time estimated by the analytical model has been validated using DPM multiphase model in FLUENT for the case of 4 mm thick carbon steel strip (base input condition). The results are summarized in Table 3 and compared with the predictions of analytical model. Fig. 5 pictorially compares droplet evaporation time as a function of droplet diameter using analytical model and CFD model. The simulated values of droplet evaporation time agree closely with the predictions of the analytical model. Small discrepancy can be attributed to error in estimation of vapor film thickness. It is to be noted that the predictions of the CFD model exceeds the predictions of the analytical model for all values of droplet diameter. Pilot-plant studies are needed to validate whether the analytical model or the CFD model better represents the actual droplet evaporation time under conditions identical to Runout Table cooling. Either model can then be tuned to fit the measured droplet evaporation time.

Fig. 6 depicts the progressive shrinkage of droplet size with time for a 70 μm droplet which is the critical droplet size for a 4 mm thick carbon steel strip. Datapoints marked by solid squares represent the predictions of analytical model whereas datapoints marked by solid triangles represent the predictions of CFD model. It may be recalled that the analytical model predicts that at time $t = 0$ ms, diameter of the hemispherical droplet is 88.2 μm [using Eq. (5)] and not 70 μm since the spherical droplet gets flattened

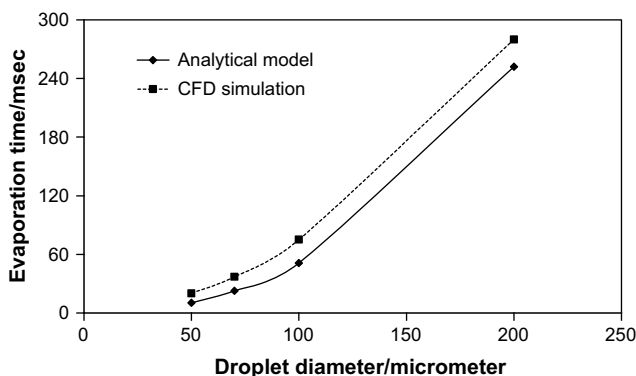


Fig. 5. Validation of analytical model using CFD simulation.

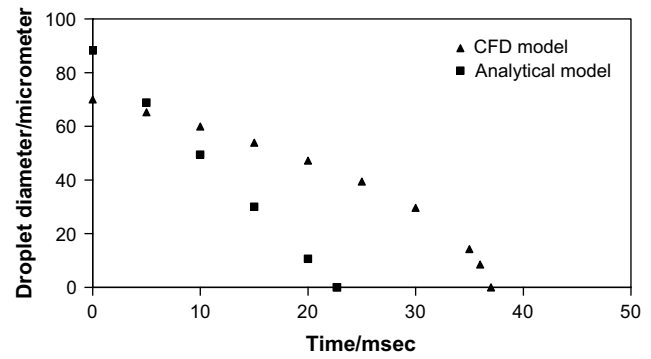


Fig. 6. Variation of droplet diameter with time for 70 μm droplet.

upon impingement on the hot steel strip surface. Since the CFD model do not consider change of droplet shape upon impingement, the curve for CFD model starts at 70 μm . Moreover, the analytical model – unlike CFD model – predicts that droplet diameter decreases linearly with time since the vapor film thickness is assumed to remain constant during the course of droplet vaporization.

Apart from CFD validation, droplet evaporation time estimated by the present analytical model has also been compared with the predictions of another analytical model developed by Zhang and Gogos [12]. For a water droplet of diameter 100 μm impinging on a hot surface at 600 $^{\circ}\text{C}$, the model in [12] predicts evaporation time as 0.12 s whereas the present analytical model predicts 0.10 s. Evidently the matching is pretty close considering the differences in the two models. However it deserves to be mentioned that the model of Zhang and Gogos is much more detailed than the present analytical model including general flow field solution accounting for radially outward evaporation-induced velocity at liquid–gas interface. In addition to flow, energy equation and species equation were also solved with the boundary condition at the droplet interface coupling the temperature, species and flow field. For simplicity, the present analytical model has not considered the fluid mechanics point of view and used Bianco correlation to estimate vapor film thickness. This is justifiable since the emphasis of the present study is on heat transfer with phase change keeping in mind a specific application – Ultra Fast Cooling in Runout Table of Hot Strip Mill. Close matching of results further justifies the simplified modeling approach in the present study.

4. Conclusion

Spray evaporative cooling as an alternative to conventional laminar jet impingement cooling has potential to achieve the anomalously high strip cooling rate of Ultra Fast Cooling in Runout Table of Hot Strip Mill. In the present study, heat transfer involved in spray evaporative cooling has been estimated from single droplet studies since a spray is equivalent to a multi-droplet array of liquid at low spray flux density. Based on this premise, an analytical expression of droplet evaporation time has been developed from fundamental heat transfer perspective which is used to estimate strip cooling rate. The analytical model developed predicts that it is indeed possible to achieve the anomalously high strip cooling rate of Ultra Fast Cooling in a 4 mm thick steel strip by spray evaporative cooling provided droplet size is reduced to 70 μm . Effect of steel strip thickness on critical droplet size to achieve Ultra Fast Cooling has been quantified. It is observed that smaller droplets may be capable of providing the increased cooling load of Ultra Fast Cooling for thicker steel strips. Droplet evaporation time estimated by the

analytical model has been validated using CFD simulation with Discrete Phase Model. The simulated results agree closely with the analytical calculations. Small discrepancy between simulated and analytical results can be attributed to error in estimation of vapor film thickness. Future work should be directed at pilot-plant studies to experimentally validate the capability of spray evaporative cooling to achieve Ultra Fast Cooling in Runout Table of Hot Strip Mill by reducing droplet size.

References

- [1] R.P. Selvam, L. Lin, R. Ponnappan, Direct simulation of spray cooling: Effect of vapor bubble growth and liquid droplet impact on heat transfer, *Int. J. Heat Mass Transfer* 49 (2006) 4265–4278.
- [2] A. Lucas, P. Simon, G. Bourdon, J.C. Herman, P. Riche, J. Neutjens, P. Harlet, Metallurgical aspects of ultra fast cooling in front of the down-coiler, *Steel Research* 75 (2) (2004) 139–146.
- [3] J.C. Herman, Impact of new rolling and cooling technologies on thermo-mechanically processed steels, *Ironmaking & Steelmaking* 28 (2) (2001) 159–163.
- [4] N. Hatta, H. Osakabe, Numerical modeling for cooling process of a moving hot plate by a laminar water curtain, *ISIJ International* 29 (11) (1989) 919–925.
- [5] H. Fujimoto, H. Takuda, N. Hatta, R. Viskanta, Numerical simulation of transient cooling of a hot solid by an impinging free surface jet, *Numerical Heat Transfer Part A* 36 (1999) 767–780.
- [6] W. Timm, K. Weinzierl, A. Leipertz, Heat transfer in subcooled jet impingement boiling at high wall temperatures, *Int. J. Heat Mass Transfer* 46 (2003) 1385–1393.
- [7] A.T. Hauksson, D. Fraser, V. Prodanovic, I. Samarasekera, Experimental study of boiling heat transfer during subcooled water jet impingement on flat steel surface, *Ironmaking & Steelmaking* 31 (1) (2004) 51–56.
- [8] A. Biance, C. Clanet, D. Quere, Leidenfrost drops, *Physics of Fluids* 15 (6) (2003) 1632–1637.
- [9] T.Y. Xiong, M.C. Yuen, Evaporation of a liquid droplet on a hot plate, *Int. J. Heat Mass Transfer* 34 (7) (1991) 1881–1894.
- [10] I. Michiyoshi, K. Makino, Heat transfer characteristics of evaporation of a liquid droplet on heated surfaces, *Int. J. Heat Mass Transfer* 21 (1978) 605–613.
- [11] Fluent Release 6.2.16 User's Guide, Fluent Inc, Lebanon, New Hampshire.
- [12] S. Zhang, G. Gogos, Film evaporation of a spherical droplet over a hot surface: fluid mechanics and heat/mass transfer analysis, *J. Fluid Mech.* 222 (1991) 543–563.
- [13] M.N. Ozisik, *Heat Transfer A Basic Approach* Int ed., McGraw-Hill, Singapore, 1985.